

Regularized calculation of the retarded Green function in Schwarzschild spacetime

Marc Casals,^{1,2,*} Brien C. Nolan,^{3,†} Adrian C. Ottewill,^{2,‡} and Barry Wardell^{2,§}

¹*Centro Brasileiro de Pesquisas Físicas (CBPF), Rio de Janeiro, CEP 22290-180, Brazil.*

²*School of Mathematics and Statistics, University College Dublin, Belfield, Dublin 4, Ireland.*

³*School of Mathematical Sciences, Dublin City University, Glasnevin, Dublin 9, Ireland.*

(Dated: March 4, 2022)

The retarded Green function for linear field perturbations of black hole spacetimes is notoriously difficult to calculate. One of the difficulties is due to a Dirac- δ divergence that the Green function possesses when the two spacetime points are connected by a “direct” null geodesic. We present a procedure which notably aids its calculation in the case of Schwarzschild spacetime by separating this direct δ -divergence from the remainder of the retarded Green function. More precisely, the method consists of calculating the multipolar ℓ -modes of the direct δ -divergence and subtracting them from the corresponding modes of the retarded Green function. We illustrate the usefulness of the method with some specific calculations in the case of the scalar Green function and self-field for a point scalar charge in Schwarzschild spacetime.

I. INTRODUCTION

Linear field perturbations of black hole spacetimes obey a wave equation. The retarded Green function (GF) of this equation is an important function of two spacetime points, as it serves to evolve any initial field data to its future. Certain problems require knowing the retarded Green function *globally*, i.e., for points arbitrarily separated. For example, the self-field on a point particle moving on a background black hole spacetime can be expressed in terms of an integral of the GF over the past worldline of the particle. The self-force can then be obtained as a derivative of the self-field (see [1, 2] for reviews). Also, within the different setting of relativistic quantum information, the probability of a particle detector being excited by a field emitted by another detector moving on a curved background can be expressed as a (double) integral of the GF¹ (see, e.g., [3, 4]).

Calculating the GF on a black hole background is no easy endeavour. One of the difficulties lies in the fact that the GF diverges when the two spacetime points are connected via a null geodesic [5, 6]. The so-called Hadamard form shows that, for the case of “direct” null geodesics (i.e., for null geodesics which have not orbited around the black hole and so, in particular, have not encountered a caustic), this divergence is of a Dirac- δ type [1, 7, 8]. The term in the Hadamard form which contains this direct divergence is called the *direct part*. In a practical calculation, where the GF is only calculated *approximately* to within a desired accuracy, this direct divergence is typically smeared out and “contaminates” the evaluation of the GF even when the spacetime points are *timelike*-separated.

In this paper, we present a simple but very useful idea for facilitating the practical evaluation of the GF on a static and spherically-symmetric spacetime (including, for example, the Schwarzschild black hole spacetime) via a multipolar ℓ -mode decomposition (as used, for example, in Refs. [9, 10]). Within such a decomposition, the divergences of the GF when the spacetime points are null-separated manifest as divergences of the infinite sum over ℓ -modes [11]. Since, in a practical calculation, one must truncate the sum at a *finite* number of modes, the divergences of the computed GF are inevitably spread out. This implies, in particular, that when the points are close to being connected by a direct null geodesic, a large number of ℓ -modes are required in the sum in order to avoid contamination from the direct part. Our proposal is to obtain the ℓ -modes of the direct part in the Hadamard form and subtract them from the ℓ -modes of the full GF, prior to carrying out the ℓ -sum. The resulting object is, thus, essentially, the full GF *minus* the direct part. Since this object does not diverge when the points are connected by a direct null geodesic, its ℓ -sum converges much faster for points close to being connected by such a geodesic.

* mcasals@cbpf.br, marc.casals@ucd.ie

† brien.nolan@dcu.ie

‡ adrian.ottewill@ucd.ie

§ barry.wardell@ucd.ie

¹ Even though in this setting of relativistic quantum information the field is quantized, to *leading* order in the coupling between the detectors and the field, the signal strength depends only on the *retarded* Green function and so it does not depend on the quantum state of the field.

The contribution from the direct part is, in fact, not needed for certain problems such as the self-force problem (in this case, the direct part is “regularized away”). For problems where this contribution is needed, such as in the relativistic quantum information setting, it can be calculated separately using an alternative method which does not involve an ℓ -mode decomposition. Although we present the method explicitly for the case of a massless scalar field on Schwarzschild spacetime, it can readily be extended to fields of non-zero spin. We illustrate the usefulness of our proposal with a practical calculation of the scalar GF and self-field in Schwarzschild spacetime. Our example shows that many fewer ℓ -modes are required to achieve a certain accuracy when our proposal of subtracting the ℓ -modes of the direct part is used, thus greatly facilitating the evaluation of the ℓ -sum.

This paper is organized as follows. In Sec. II we present the GF for the wave equation in curved spacetimes and the difficulties with its practical evaluation in Schwarzschild spacetime. In Sec. III we present our proposal for facilitating the evaluation of the GF. We implement this proposal specifically in the case of the calculation of the scalar GF and self-field in Sec. IV. We finish in Sec. V with possible extensions of the application of our method. In the appendices we derive small-coordinate expansions of the ℓ -modes of the retarded Green function and of its direct part.

We use geometric units $c = G = 1$ and metric signature $(-+++)$ throughout this work.

II. GREEN FUNCTION

Let us consider a massless scalar field propagating on a curved background spacetime, with the field satisfying the Klein-Gordon equation. The corresponding retarded Green function (GF) satisfies the Klein-Gordon equation with a four-dimensional (invariant) Dirac- δ distribution as the source:

$$\square_x G_{\text{ret}}(x, x') = -4\pi \frac{\delta_4(x - x')}{\sqrt{-g(x)}}, \quad (1)$$

where x' and x are two spacetime points² and \square_x is the D'Alembertian with respect to x . The GF obeys causal boundary conditions: it is equal to zero if x' does not lie in the causal past of x .

There exists an analytical expression for the GF, the so-called *Hadamard form*, which is valid when x' is in a local neighbourhood of x . More precisely, x' must lie in a *normal neighbourhood* $\mathcal{N}(x)$ of x : a region $\mathcal{N}(x)$ containing x such that every $x' \in \mathcal{N}(x)$ is connected to x by a *unique* geodesic which lies in $\mathcal{N}(x)$. The Hadamard form is [1, 7, 8]:

$$G_{\text{ret}}(x, x') = [U(x, x')\delta(\sigma) + V(x, x')\theta(-\sigma)]\theta(\Delta t), \quad (2)$$

where $U(x, x')$ and $V(x, x')$ are regular, real-valued biscalars, $\Delta t \equiv t - t'$ and t is a time coordinate. Here, $\sigma = \sigma(x, x')$ is Synge's world-function [12], which is equal to one-half of the squared distance along the (unique) geodesic connecting x and x' . This means that σ is negative/zero/positive whenever that geodesic is timelike/null/spacelike. Eq. (2) exhibits a Dirac- δ divergence at $\sigma = 0$, i.e., when the spacetime points are connected by a “direct” null geodesic or else when they coincide (i.e., $x' = x$). We thus refer to $G_{\text{d}}(x, x') \equiv U\delta(\sigma)\theta(\Delta t)$, which only has support when the points are null separated, as the “direct part”, and to $V\theta(-\sigma)\theta(\Delta t)$, which also has support when the points are timelike separated, as the “tail part”. The “direct biscalar” $U(x, x')$ is related to the so-called van Vleck determinant Δ [13–15] by $U(x, x') = \Delta^{1/2}(x, x')$ and satisfies a transport equation along the unique geodesic joining x and x' . In turn, the “tail biscalar” $V(x, x')$ satisfies the homogeneous Klein-Gordon equation.

As mentioned, the Hadamard form is only valid in a local neighbourhood, while one may need the GF for arbitrarily separated points in the spacetime. When the background spacetime is spherically-symmetric, it is useful to carry out a multipolar decomposition of the GF, which is valid *globally*, as

$$G_{\text{ret}}(x, x') = \frac{1}{r r'} \sum_{\ell=0}^{\infty} (2\ell + 1) P_{\ell}(\cos \gamma) G_{\ell}^{\text{ret}}(r, r'; \Delta t), \quad (3)$$

where $\gamma \in [0, \pi]$ is the angle separation between x and x' and r is a radial coordinate. The multipolar modes G_{ℓ}^{ret} satisfy a Green function equation in $(1 + 1)$ -dimensions. These modes can be calculated in a variety of ways –

² As is common, we blur the distinction between points (e.g. x and x') and their coordinates given a global coordinate system on the exterior Schwarzschild spacetime under consideration.

for example, as a Fourier integral over real frequencies [16]; as a sum over quasi-normal modes plus a branch cut integral [9, 17]; or via a numerical integration of the (1 + 1)-D Green function equation that they satisfy [10, 18].

When calculating the GF via Eq. (3), the Dirac- δ divergence at $\sigma = 0$ arises from a divergence in the infinite ℓ -mode sum [11]. In a practical calculation, however, it is not possible to include an infinite number of ℓ -modes and so the infinite sum must be truncated at some finite upper cutoff. As a consequence of this finite cutoff, spurious oscillations appear, but these can be smoothed out via the introduction of a factor which decays fast for large ℓ [9, 19]. The finite cutoff, including a smoothing factor, effectively means that the sharp $\delta(\sigma)$ divergence is not exactly captured and, instead, one obtains an element of a δ -convergent sequence. For example, in this paper, we chose $e^{-\ell^2/(2\ell_{cut}^2)}$, for some choice of $\ell_{cut} \in \mathbb{R}$, as the smoothing factor, and then the δ -convergent sequence is a Gaussian distribution centered at $\sigma = 0$; we shall henceforth refer to the δ -convergent sequence as a Gaussian distribution for simplicity. This means that the approximate GF resulting from the finite cutoff and smoothing factor is highly “contaminated” by the Gaussian distribution at points near $\sigma = 0$. Therefore, in a normal neighbourhood $x' \in \mathcal{N}(x)$, even though the *exact* $G_{ret}(x, x')$ is equal to $V(x, x')$ for points x' timelike-separated from x , the *approximate* $G_{ret}(x, x')$ may differ considerably from the correct value given by $V(x, x')$ for points near $\sigma = 0$. This approximation to the GF becomes worse the closer the points are to $\sigma = 0$.

In previous work [9, 10, 20–22], the above problem of obtaining the GF for points “near” $\sigma = 0$ was addressed by calculating the GF in that regime, not via Eq. (3), but rather via a direct evaluation of $V(x, x')$. Such evaluation can be achieved, for example, using the following multiple power series [23]:

$$V(x, x') = \sum_{i,j,k=0}^{\infty} v_{ijk}(r)(t-t')^{2i}(1-\cos\gamma)^j(r-r')^k, \quad (4)$$

for some coefficients v_{ijk} that can be determined. Again, in a practical calculation, one must stop the sums in (4) at some finite upper limits, thus yielding an approximation to the regular bitensor $V(x, x')$. The approximation becomes worse the further the points are from each other in the sense of large coordinate increments (i.e. large $|t-t'|$, $|r-r'|$ and/or γ)³. The aim is to match the calculation of $V(x, x')$ via (4), with the sums truncated, to the mode-sum calculation via (3), also with the sum truncated, in a region where both approximations are accurate enough (i.e., the truncation error is smaller than a desired accuracy). The region where the approximation to $V(x, x')$ is accurate enough is called the quasi-local (QL) region, and the region where the approximation to the mode sum (3) is accurate enough is called the Distant Past (DP).

This approach encounters a fundamental challenge, namely that the existence of an overlap between the QL and the DP regions is not guaranteed. In Ref. [9, 10] it was shown that, by using a Padé resummation of the QL approximation, the two regions do overlap for many cases of relevance to the self-force problem in Schwarzschild spacetime. However, the overlapping region was found to be often quite small, and ultimately the matching between QL and DP regions was found to be the dominant limitation in achieving robust (i.e. valid in a wide variety of scenarios) and accurate results. In order to increase the chances of having a region of overlap, or to improve agreement in an overlapping region, one has two options: (i) to improve the calculation of $V(x, x')$ so that the QL approximation becomes more accurate in a larger region; (ii) to improve the calculation via (3) so that the DP approximation becomes more accurate in a larger region. The former has a fundamental limitation, which is that $V(x, x')$ diverges at the edge of the normal neighbourhood, and so any power series approximation will struggle to accurately represent it near this divergence. The latter saw some improvement by going from a quasinormal mode sum approximation [9], which is known to have very poor convergence when the points are close together, to a time domain method for computing G_{ret}^{ℓ} [10]. However, this improvement did not address the problem of poor convergence of the ℓ -sum in the DP contribution. In this paper we present a method for addressing this problem, largely eliminating it.

III. REGULARIZED CALCULATION OF THE GREEN FUNCTION

As mentioned, the calculation of the GF via (3) encounters problems for points near $\sigma = 0$ because the truncation of the sum (in combination with the introduction of a smoothing factor) effectively turns the Dirac- δ divergence exhibited in (2) into a widespread Gaussian distribution. One might expect that the approximation will improve if

³ We note that such points where the truncated approximation to Eq. (4) becomes worse may still be close to $\sigma = 0$, as well as including points for which $\sigma(x, x')$ is large.

we calculate a multipolar decomposition of the result of subtracting the direct part $G_d(x, x') \equiv U\delta(\sigma)\theta(\Delta t)$ from the GF. The reason is that the quantity resulting from such subtraction (which is equal to $V\theta(-\sigma)\theta(\Delta t)$ when $x' \in \mathcal{N}(x)$) is finite at $\sigma = 0$. In order to achieve this, in this section we shall subtract the multipolar modes of the direct part G_d from the multipolar modes G_ℓ^{ret} of the full GF. For this purpose, it is very convenient to follow Ref. [11].

From now on we focus on Schwarzschild space-time with mass M , and will work in Schwarzschild coordinates $\{t, r, \theta, \varphi\}$. First, we make the conformal transformation

$$d\hat{s}^2 \equiv r^{-2}ds^2 = ds_2^2 g + d\Omega_2^2, \quad (5)$$

where ds^2 and $d\Omega_2^2$ are the line-elements in, respectively, Schwarzschild spacetime and the unit 2-sphere \mathbb{S}^2 , and we have defined

$$ds_2^2 \equiv \frac{f}{r^2} (-dt^2 + f^{-2}dr^2), \quad (6)$$

with $f \equiv 1 - 2M/r$. We call the 4-D spacetime with the metric (5) the conformal Schwarzschild spacetime \mathcal{M}_\times , and we call the spacetime with metric (6) the 2-D conformal spacetime \mathcal{M}_2 . This 2-D spacetime was studied in [24], where it was proven to be a causal domain (i.e., \mathcal{M}_2 is geodesically convex and it obeys a certain causality condition) [8]. As a consequence, both the world-function and the Hadamard form for the Green function in \mathcal{M}_2 are valid globally in this 2-D spacetime [8].

Since Eq. (5) is a conformal transformation, if we consider a conformally-coupled scalar field we have that the GF in Schwarzschild spacetime is [8, 25]

$$G_{\text{ret}}(x, x') = \frac{1}{r \cdot r'} \hat{G}_R(x, x'), \quad (7)$$

where $\hat{G}_R(x, x')$ is the GF for the Klein-Gordon equation in conformal Schwarzschild spacetime. Both GF's G_{ret} and \hat{G}_R admit the Hadamard form (2); we denote the biscalars in Schwarzschild spacetime as in (2), whereas we denote the biscalars in the conformal Schwarzschild spacetime with the corresponding hatted symbols, so that, in particular, $\hat{\Delta}(x, x')$ and $\hat{\sigma}$ denote, respectively, the van Vleck determinant and the world function in \mathcal{M}_\times . By comparing the direct parts of the Hadamard forms for the two GF's, we have that

$$G_d(x, x') = \Delta^{1/2}(x, x')\delta(\sigma)\theta(\Delta t) = \frac{\hat{\Delta}^{1/2}(x, x')\delta(\hat{\sigma})\theta(\Delta t)}{r \cdot r'}. \quad (8)$$

Equation (8) holds because $\sigma(x, x') = 0$ if and only if $\hat{\sigma}(x, x') = 0$, which follows from the invariance properties of null geodesics under conformal transformations.

As mentioned, the Hadamard form (2) is only valid in normal neighbourhoods [we will later explicitly determine the normal neighbourhood of an arbitrary point in \mathcal{M}_\times : the result is given in Eq. (16)]. A great advantage of the transformation in (5) is that the conformal Schwarzschild spacetime is a direct product: the manifold has the form $\mathcal{M}_\times = \mathcal{M}_2 \times \mathbb{S}^2$, with line element given by (5) with (6). Writing coordinates on the 4-D spacetime \mathcal{M}_\times as $x^\alpha = (x^A, x^a)$ where $x^A, A = 0, 1$ are coordinates on \mathcal{M}_2 and $x^a, a = 2, 3$ are coordinates on the 2-sphere \mathbb{S}^2 , we see that the metric tensor decomposes as ⁴

$$g_{\alpha\beta} = \begin{pmatrix} g_{AB}(x^C) & 0 \\ 0 & g_{ab}(x^c) \end{pmatrix}, \quad (9)$$

while the (Levi-Civita) connection coefficients decompose as

$$\Gamma^A_{\beta\gamma}(x^\delta) = \begin{pmatrix} \Gamma^A_{BC}(x^D) & 0 \\ 0 & 0 \end{pmatrix}, \quad \Gamma^a_{\beta\gamma}(x^\delta) = \begin{pmatrix} 0 & 0 \\ 0 & \Gamma^a_{bc}(x^d) \end{pmatrix}. \quad (10)$$

It then follows that there is a one-to-one correspondence between geodesics of the spacetime \mathcal{M}_\times and ‘products’ of geodesics on \mathcal{M}_2 and \mathbb{S}^2 . That is, a parametrized curve $\lambda : x^\alpha = x^\alpha(s) = (x^A(s), x^a(s))$ is a geodesic of the spacetime \mathcal{M}_\times if and only if $\mu : x^A = x^A(s)$ and $\nu : x^a = x^a(s)$ are geodesics on \mathcal{M}_2 and \mathbb{S}^2 respectively. (We will say that μ

⁴ Greek letters as indices denote indices in the 4-D spacetime, capital Latin letters indices on \mathcal{M}_2 and small Latin letters indices on \mathbb{S}^2 .

and ν lift to yield λ , which *projects* to yield μ and ν .) As noted above, (\mathcal{M}_2, g_{AB}) is geodesically convex: there is a unique geodesic between any pair of points of \mathcal{M}_2 . Then the world function σ_2 on \mathcal{M}_2 is defined globally and may be written as

$$\sigma_2(x^A, x^{A'}) = \frac{\epsilon}{2}\eta^2, \quad (11)$$

where $\epsilon = -1, 0, +1$ for timelike, null and spacelike separations in \mathcal{M}_2 and η is proper time, zero and proper distance respectively along the corresponding timelike, null and spacelike geodesics. (By convention, $\eta \geq 0$ along a future-directed causal curve from $x^{A'}$ to x^A .) Below Eq. (3), we already defined $\gamma = \gamma(x^a, x^{a'}) \in [0, \pi]$, which we can here understand more explicitly as the *geodesic separation* of x^a and $x^{a'}$: the proper length of the *shortest* geodesic from x^a to $x^{a'}$. We distinguish this from the *geodesic distance* $\gamma_\nu(x^a, x^{a'})$ which measures the length of a geodesic ν from x^a to $x^{a'}$. This may be arbitrarily long (by running around the sphere multiple times) and may also run in the direction opposite to that of the shortest geodesic. Note that we must have either

$$\gamma_\nu(x^a, x^{a'}) = \gamma + 2n\pi \quad (12)$$

or

$$\gamma_\nu(x^a, x^{a'}) = 2n\pi - \gamma \quad (13)$$

for some $n \in \mathbb{N}$.

The question of uniqueness of geodesics connecting points of the 4-D spacetime is then easily resolved [11]. Consider two points $x = (x^A, x^a)$ and $x' = (x^{A'}, x^{a'})$ of the spacetime \mathcal{M}_\times , where x^a and $x^{a'}$ are non-antipodal points on \mathbb{S}^2 . There is a unique geodesic μ of \mathcal{M}_2 connecting x^A and $x^{A'}$, and generically there are two countably infinite families of geodesics on \mathbb{S}^2 connecting x^a and $x^{a'}$. Among these there is a unique shortest geodesic ν_0 for which $\gamma_{\nu_0}(x^a, x^{a'}) = \gamma(x^a, x^{a'})$. In the case of a null geodesic, the pair μ, ν_0 lift to what we have referred to as the *direct* null geodesic connecting points of Schwarzschild spacetime (in fact the conformal transformation from \mathcal{M}_\times to Schwarzschild is also required). These geodesics on \mathcal{M}_2 and \mathbb{S}^2 lift to give geodesics on the spacetime \mathcal{M}_\times as noted above, and so spacetime points are (generically) connected by two countably infinite families of geodesics. Among these, the geodesic formed by lifting μ and ν_0 is distinguished. We can then define a 2-point function on the spacetime \mathcal{M}_\times by

$$\hat{\sigma}(x, x') = \frac{\epsilon}{2}\eta^2 + \frac{1}{2}\gamma^2. \quad (14)$$

Care is needed in interpreting this as the world function of the spacetime as $\hat{\sigma}$ measures one half the square of the geodesic distance (appropriately signed) along the unique geodesic whose projection into \mathbb{S}^2 yields ν_0 . This is not the only geodesic from x to x' . However, this situation changes when we restrict to *causal* geodesics. So consider a causal geodesic $\lambda : x^a = x^a(s)$ from x to x' in \mathcal{M}_\times . This projects to a causal geodesic $\mu : x^A = x^A(s)$ on \mathcal{M}_2 and a spacelike geodesic $\nu : x^a = x^a(s)$ on \mathbb{S}^2 . Then one half the square of the geodesic distance from x to x' along λ is given by

$$\hat{\sigma}_\lambda(x, x') = \frac{\epsilon}{2}\eta^2(x^A, x^{A'}) + \frac{1}{2}\gamma_\nu^2(x^a, x^{a'}). \quad (15)$$

This must be non-positive, and so there is a *finite* number of geodesics ν which allow for λ to be causal, among which must be the shortest spacelike geodesic ν_0 . This leads us to a crucial point: Suppose that $x = (x^A, x^a), x' = (x^{A'}, x^{a'}) \in \mathcal{M}_\times$ are connected by a causal geodesic which is not a radial null geodesic ($\gamma(x^a, x^{a'}) \neq 0$). (It is easily verified that spacetime points connected by a radial null geodesic are connected by a unique causal geodesic.) Then η , the proper time separation of (necessarily) timelike separated points x^A and $x^{A'}$ in \mathcal{M}_2 is fixed, and we must have $\eta(x^A, x^{A'}) \geq \gamma(x^a, x^{a'}) = \gamma_{\nu_0}$. The next shortest geodesic ν_1 on \mathbb{S}^2 connecting x^a and $x^{a'}$ lies on the great circle connecting these points, running in the direction opposite to that of ν_0 , and so has $\gamma_{\nu_1} = 2\pi - \gamma_{\nu_0} = 2\pi - \gamma$. The corresponding geodesic $\lambda_1 = (\mu, \nu_1)$ is causal if and only if $\eta \geq 2\pi - \gamma$. If λ_1 is not causal, then no further spacelike geodesic ν_* of \mathbb{S}^2 from x^a to $x^{a'}$ - which would have $\gamma_{\nu_*} > \gamma_{\nu_1}$ - will yield a causal geodesic $\lambda_* = (\mu, \nu_*)$ of \mathcal{M}_\times . Hence the inequalities $\eta \geq \gamma$ and $\eta \geq 2\pi - \gamma$ are the necessary and sufficient conditions for the existence of multiple causal geodesics from x to x' . Note that the conditions that both $\lambda = (\mu, \nu_0)$ and $\lambda_1 = (\mu, \nu_1)$ are causal imply that $\eta \geq \pi$. For $\eta(x^A, x^{A'}) < 2\pi - \gamma$ and given $x = (x^A, x^a)$, there is a non-trivial open set of points x' for which x and x' are connected by a unique causal geodesic. In order to obtain an open set of points x' connected to x by a unique geodesic (regardless of causal character) which remains within that set, we must exclude the point $x^{a'} \in \mathbb{S}^2$ antipodal

to x^a , which we did not consider in the whole argument above. That is, each $x = (x^A, x^a) \in \mathcal{M}_\times$ has a (maximal) normal neighbourhood $\mathcal{N}(x)$ of the form

$$\mathcal{N}(x) = \{(x^{A'}, x^{a'}) \in \mathcal{M}_\times : \eta(x^A, x^{A'}) < 2\pi - \gamma(x^a, x^{a'}), \gamma(x^a, x^{a'}) < \pi\}. \quad (16)$$

Then, for each $x \in \mathcal{M}_\times$, (14) defines the world function $\hat{\sigma}(x, x')$ on $\mathcal{N}(x)$, the retarded Green function $\hat{G}_R(x, x')$ assumes the Hadamard form corresponding to (2) and the direct part takes the form given in (8). Existence, uniqueness and the corresponding form to Eq. (2) for \hat{G}_R follow from Theorem 4.5.1 and Corollary 5.1.1 of [8]⁵.

Another advantage of conformal Schwarzschild spacetime being a direct product is that its van Vleck determinant may be factorized as (e.g., [26])

$$\hat{\Delta}(x, x') = \Delta_{2d}(x^A, x^{A'}) \Delta_{\mathbb{S}^2}(\gamma), \quad (17)$$

where Δ_{2d} and

$$\Delta_{\mathbb{S}^2} \equiv \frac{\gamma}{\sin \gamma} \quad (18)$$

are the van Vleck determinants in, respectively, \mathcal{M}_2 and \mathbb{S}^2 .

After determining normal neighbourhoods in \mathcal{M}_\times and the explicit γ -dependence of the direct part $G_d = U\delta(\sigma)\theta(\Delta t)$ in Schwarzschild spacetime, we can now proceed to calculate the multipolar modes of this direct part. From Eqs. (8), (17) and (18), these multipolar modes are given by

$$\begin{aligned} G_\ell^d(r, r'; \Delta t) &\equiv \frac{r r'}{2} \int_{-1}^{+1} d(\cos \gamma) P_\ell(\cos \gamma) \Delta^{1/2}(x, x') \delta(\sigma) \theta(\Delta t) \\ &= \frac{\theta(\Delta t)}{2} \Delta_{2d}^{1/2}(x^A, x^{A'}) \int_{-1}^{+1} d(\cos \gamma) P_\ell(\cos \gamma) \left(\frac{\gamma}{\sin \gamma} \right)^{1/2} \delta(\hat{\sigma}). \end{aligned} \quad (19)$$

Using (14), we have that

$$G_\ell^d(r, r'; \Delta t) = \frac{\theta(\Delta t)}{2} \theta(\pi - \eta) \Delta_{2d}^{1/2}(x^A, x^{A'}) P_\ell(\cos \eta) \left(\frac{\sin \eta}{\eta} \right)^{1/2}. \quad (20)$$

In evaluating Eq. (19), we note that $\eta \geq 0$ since $\Delta t \geq 0$. The presence of the Heaviside function $\theta(\pi - \eta)$ can be understood as follows. For a fixed $x \in \mathcal{M}_\times$, G_ℓ^d is defined only for $x' \in \mathcal{N}(x)$ [see Eq. (16)] and has support only when $\hat{\sigma} = 0$. But for $\eta > \pi$ and $x' \in \mathcal{N}(x)$, we have $\hat{\sigma}(x, x') < 0$ and so $G_\ell^d = 0$. It is worth noting that G_ℓ^d has compact support in η due to the presence of the two Heaviside θ 's in Eq. (20). It is trivial to check that the original direct part, Eq. (8), is recovered by summing these modes as in

$$G_d(x, x') = \frac{1}{r r'} \sum_{\ell=0}^{\infty} (2\ell + 1) P_\ell(\cos \gamma) G_\ell^d(r, r'; \Delta t). \quad (21)$$

It is worth pointing out that $G_d(x, x')$ is defined (via Eq. (8)) only for $x' \in \mathcal{N}(x)$. However, using the expression for G_ℓ^d in (20), the sum on the right hand side of (21) yields a quantity defined everywhere on \mathcal{M}_\times , which is identically zero for x' outside $\mathcal{N}(x)$.

Via Eq. (20) we have thus reduced the calculation of the direct multipolar modes G_ℓ^d in Schwarzschild spacetime to the calculation of the distance η and the van Vleck determinant Δ_{2d} in \mathcal{M}_2 . Unfortunately, closed form expressions for these quantities are not known and so they must be calculated either: (i) numerically, as was done in Ref. [24], by solving transport equations [27] along the unique geodesic that joins the two points in \mathcal{M}_2 ; or (ii) using series approximations valid for small separations of the points (see Appendix A).⁶

⁵ The relevant results require that (x, x') lie in a causal domain Ω of the spacetime, for which all pairs of points of Ω are joined by a unique geodesic which lies in Ω . We can construct the required geodesically convex regions by excluding a semi-great circle of points from \mathbb{S}^2 rather than a single point. Since the base point x is fixed throughout, we can keep the discussion in terms of normal neighbourhoods rather than causal domains.

⁶ In the simpler cases of flat and Nariai spacetimes, the equivalent of these quantities in their corresponding 2-D conformal spacetimes are known in closed form and so the multipolar modes can also be obtained in closed form – see Appendix A in [11].

Summarizing, our method replaces the calculation of the retarded Green function in (3) by that of the following “non-direct” part of the retarded Green function,

$$G_{\text{nd}}(x, x') \equiv \frac{1}{r r'} \sum_{\ell=0}^{\infty} (2\ell + 1) P_{\ell}(\cos \gamma) (G_{\ell}^{\text{ret}}(r, r'; \Delta t) - G_{\ell}^{\text{d}}(r, r'; \Delta t)). \quad (22)$$

By construction, it is

$$G_{\text{nd}}(x, x') = G_{\text{ret}}(x, x') - G_{\text{d}}(x, x') = \begin{cases} G_{\text{ret}}(x, x') - U(x, x')\delta(\sigma)\theta(\Delta t) = V(x, x')\theta(-\sigma)\theta(\Delta t), & x' \in \mathcal{N}(x), \\ G_{\text{ret}}(x, x'), & x' \notin \mathcal{N}(x). \end{cases} \quad (23)$$

Therefore, $G_{\text{nd}}(x, x')$ is equal to $G_{\text{ret}}(x, x')$ unless $x' \in \mathcal{N}(x)$ and $\sigma = 0$. The advantage is that for $\sigma \neq 0$, Eq. (22) with the sum truncated at a given upper value $\ell = \ell_{\text{max}}$ approximates the exact Green function better than Eq. (3) with the sum truncated at the same upper value. In an abuse of language, we refer to G_{nd} as the “regularized Green function”.

IV. DEMONSTRATION OF THE METHOD

We now present an explicit application of our method. For demonstration purposes we focus on the case of a fixed point x with radial coordinate $r = 6M$ connected to points x' by a circular timelike geodesic. We emphasize, however, that the method works for any pair of points in Schwarzschild spacetime.

We approximate (away from $\sigma = 0$) the GF via Eq. (22) with a truncated sum. Specifically, we truncate the ℓ -sum at $\ell_{\text{max}} = 100$ and, except where otherwise specified, we include a smoothing factor $e^{-\ell^2/(2\ell_{\text{cut}}^2)}$ in the summands, with $\ell_{\text{cut}} = 20$. We evaluate G_{ℓ}^{ret} numerically using a surrogate model [28, 29] generated from numerical data produced with the method described in [10]. We also evaluate G_{ℓ}^{d} numerically by solving transport equations, as was done in Ref. [24]. At early times, $0 < t \lesssim 6M$ in this particular case, we encounter two problems:

1. The time-domain numerical approach used to produce the data for the surrogate model for G_{ℓ}^{ret} works very well almost everywhere, but breaks down very near coincidence in the 2D spacetime (which corresponds to $r = r'$ and $\Delta t = 0$, but not necessarily $\gamma = 0$) where the numerical surrogate model (which essentially uses a 2D Gaussian approximation) used causes G_{ℓ}^{ret} to tend to 0 rather than the true non-zero constant value at coincidence (as given in Eq. (24) below). This could be overcome by using a characteristic initial value formulation [18, 30, 31] in place of the Gaussian approximation.
2. There is significant cancellation between G_{ℓ}^{ret} and G_{ℓ}^{d} : both tend to the same non-zero, ℓ -independent constant as $\Delta t \rightarrow 0$ [see Eqs. (24) and (25) below]. In order to achieve the expected result that $G_{\ell}^{\text{ret}} - G_{\ell}^{\text{d}} = O(\Delta t)^6$ as $\Delta t \rightarrow 0$ [see Eq. (26) below], we require increasing cancellation between G_{ℓ}^{ret} and G_{ℓ}^{d} as Δt decreases. At sufficiently small Δt the numerical accuracy of G_{ℓ}^{ret} and G_{ℓ}^{d} is insufficient to achieve this cancellation.

We overcome both problems by using analytic, small- Δt approximations to G_{ℓ}^{ret} and G_{ℓ}^{d} in place of numerics at early times. These approximations, while only valid for small- Δt , have the advantage that they accurately reproduce the near-coincidence behaviour and can be cancelled analytically without any concerns about numerical accuracy. The details of these approximations are given in Appendices A and B. In the particular case studied here, we found the best results when using the analytic approximations for G_{ℓ}^{ret} in the region $\Delta t < 6M$ and for G_{ℓ}^{d} in the region $\Delta t < 3M$.

A. Green function

We first study the behaviour of the regularized Green function. In Fig. 1 we plot the modes G_{ℓ}^{ret} , G_{ℓ}^{d} and $G_{\ell}^{\text{ret}} - G_{\ell}^{\text{d}}$. The left plot shows that G_{ℓ}^{d} approximately agrees with G_{ℓ}^{ret} throughout much of the region where G_{ℓ}^{d} is non-zero. The right plot shows the form – including a breakdown in smoothness due to the compact support of G_{ℓ}^{d} – of the last factor in the summand in Eq. (22).

In Fig. 2 we plot the full G_{ret} [Eq. (3)], G_{nd} [Eq. (22)] and the Hadamard biscalar $V(x, x')$ [a Padé resummation of Eq. (4) — see Ref. [32] for details]. The earliest time where the solid orange line — which corresponds to the

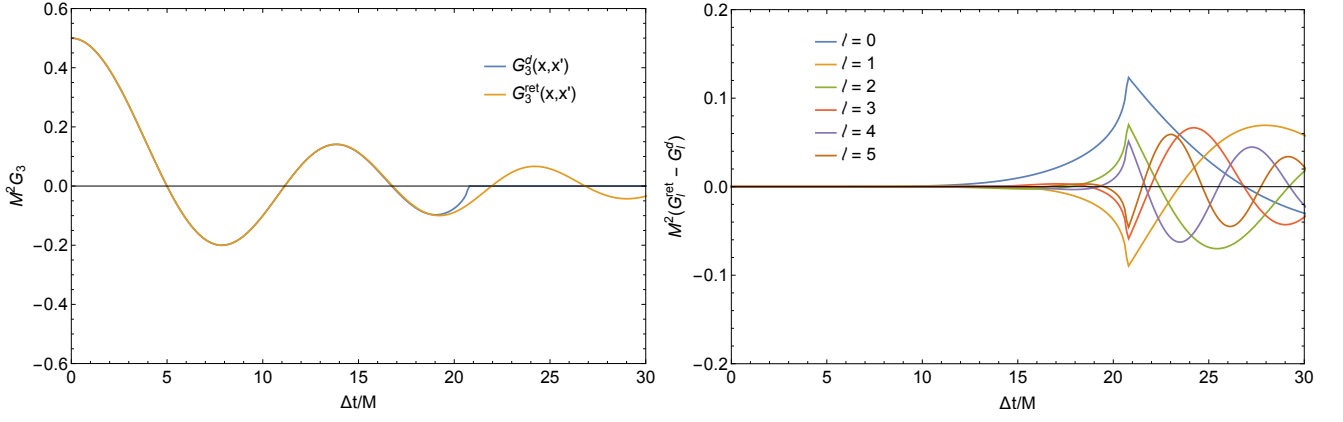


FIG. 1. Green function ℓ -modes for a scalar field on Schwarzschild spacetime as a function of time. The point x is fixed at $r = 6M$ and we vary the points x' along a circular geodesic at $r = 6M$. Left: the red curve is G_ℓ^{ret} via the method in [10] and the blue curve is G_ℓ^d from Eq. (20) for $\ell = 3$. Right: $G_\ell^{\text{ret}} - G_\ell^d$ for various ℓ values.

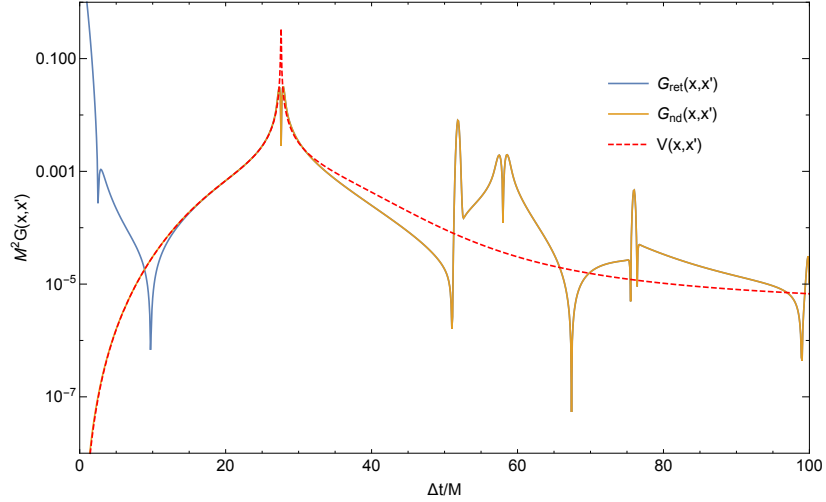


FIG. 2. Retarded Green function $G_{\text{ret}}(x, x')$ for a scalar field on Schwarzschild spacetime as a function of time. The point x is fixed at $r = 6M$ and we vary the points x' along a circular geodesic at $r = 6M$. The solid blue line shows G_{ret} , Eq. (3), computed using a truncated and smoothed multipolar mode-sum. The solid orange line shows $G_{\text{nd}}(x, x')$, Eq. (22), also computed using a truncated and smoothed multipolar mode-sum. In both cases smooth-sum parameters of $\ell_{\text{max}} = 100$ and $\ell_{\text{cut}} = 20$ were used. The dashed red line shows the Hadamard bitensor $V(x, x')$ computed from a short distance Padé-resummed Taylor series [32].

calculation of G_{nd} — spikes is where the first *non*-direct null geodesic connects x to another point x' on the worldline. Since x and this x' are connected by more than one causal geodesic (namely, the timelike worldline and the first non-direct null geodesic) and this does not happen at earlier times, this time, which is $\Delta t/M \approx 27.62$, marks the end of $\mathcal{N}(x)$ in this scenario. The other spikes in the GF, which are located at $\Delta t/M \approx 51.84, 58.05, 75.96$ and 100.09 , correspond to later non-direct null geodesics connecting x and other points x' . The GF also diverges at these points, but they are clearly outside $\mathcal{N}(x)$ and are of no relevance for the specific purposes here. What is of relevance here is that the plot shows that, near x , Eq. (22) performs much better than Eq. (3), as expected.

We end this subsection by making a comment about the behaviour at early times. Although not visible in Fig. 2, G_{nd} does not agree with $V(x, x')$ as well at early times ($\Delta t \lesssim 6M$) as it does at later times. The reason for this slight disagreement can be understood as follows. For $x' \in \mathcal{N}(x)$, the non-direct part G_{nd} is equal to $V(x, x')\theta(-\sigma)\theta(\Delta t)$ [see (23)], not $V(x, x')$. One may expect this to make no difference at early times (where $\sigma < 0$ and $\Delta t > 0$), but the fact is that we are not computing the exact G_{nd} , but an approximation to it, obtained by truncating the ℓ -sum at finite $\ell = \ell_{\text{cut}}$ and by including a smoothing factor in Eq. (22). This approximation ends up “contaminating” G_{nd} at

early times. This can be seen explicitly when carrying out a small- Δt expansion in the case of the timelike circular geodesic at $r = 6M$ that concerns us. Making use of Eqs. (A1) and (A2) and expanding Eqs. (20) and (B2) in a Taylor series about $\Delta t = 0$, we find (see Appendices A and B):

$$G_\ell^{\text{ret}} = \frac{1}{2} - \frac{3\ell^2+3\ell+1}{1296}\Delta t^2 + \frac{18\ell^4+36\ell^3+21\ell^2+3\ell-7}{6718464}\Delta t^4 - \frac{120\ell^6+360\ell^5+210\ell^4-180\ell^3-591\ell^2-441\ell-67}{87071293440}\Delta t^6 + \dots \quad (24)$$

$$G_\ell^{\text{d}} = \frac{1}{2} - \frac{3\ell^2+3\ell+1}{1296}\Delta t^2 + \frac{18\ell^4+36\ell^3+21\ell^2+3\ell-7}{6718464}\Delta t^4 - \frac{840\ell^6+2520\ell^5+1470\ell^4-1260\ell^3-4137\ell^2-3087\ell-109}{609499054080}\Delta t^6 + \dots \quad (25)$$

We thus find that these perfectly cancel through $\mathcal{O}(\Delta t^5)$, leaving a residual contribution proportional to Δt^6 ,

$$G_\ell^{\text{ret}} - G_\ell^{\text{d}} = \frac{1}{1693052928}\Delta t^6 + \dots \quad (26)$$

Comparing against the small- Δt expansion of $V(x, x')$ [using (4)], which in this case is given by

$$V(x, x') = -\frac{31}{13544423424}\Delta t^4 + \dots, \quad (27)$$

we find an apparent contradiction: $V(x, x') \sim \Delta t^4$ while $G_{\text{nd}} \sim \Delta t^6$. The resolution of this apparent contradiction is, as indicated above, that these are, in fact, not the exact same quantity but differ by a factor of $\theta(-\sigma)\theta(\Delta t)$. By considering the mode decomposition of $\theta(-\sigma)\theta(\Delta t)$ times a small- Δt expansion of $V(x, x')$, it is easily verified that this difference accounts for the difference in two orders of Δt between the two expressions. Thus, the failure of our approximation to G_{nd} to coincide with V (and so with the GF) at early times can be attributed to the smooth sum approximating the step function by a mollified version. Fortunately, this quirk has negligible effect on the results.

B. Self-field

A better approximation of the GF leads to a better approximation of the self-force and the self-field. The self-force acting on a scalar charge q moving on a worldline $z(\tau)$ on a background spacetime (with τ proper time along the geodesic), is given by $f^\mu = q\nabla^\mu\Phi_R$, where

$$\Phi_R(\tau) \equiv \lim_{\epsilon \rightarrow 0^+} \int_{-\infty}^{\tau-\epsilon} d\tau' G_{\text{ret}}(z(\tau), z(\tau')) \quad (28)$$

is the regularized self-field (the $\epsilon > 0$ in the upper limit excludes the coincidence $x' = x$, and so it excludes $\sigma = 0$ inside the normal neighbourhood). One way of carrying out the integral is to match the calculation of the GF via the multiple power series (4) in the QL region to that via the ℓ -mode sum [either Eq. (22) or Eq. (3)] in the DP. This requires a region of overlap and a choice of matching proper time τ_m :

$$\Phi_R(\tau) = \int_{-\infty}^{\tau_m} d\tau' V(z(\tau), z(\tau')) + \frac{1}{r} \lim_{\epsilon \rightarrow 0^+} \int_{\tau_m}^{\tau-\epsilon} \frac{d\tau'}{r'} \sum_{\ell=0}^{\infty} (2\ell+1) P_\ell(\cos \gamma) G_\ell^{\text{ret}}(r, r'; \Delta t), \quad (29)$$

where $r' = r'(\tau')$, $t' = t'(\tau')$, $\gamma = \gamma(\tau')$; and similarly with G_ℓ^{ret} replaced by $G_\ell^{\text{ret}} - G_\ell^{\text{d}}$. The first integral in Eq. (29) corresponds to the DP contribution and the second integral to the QL contribution.

Fig. 3 shows Φ_R for the case considered above of a scalar charge on a circular geodesic at $r = 6M$. We plot it as a function of the coordinate time t_m corresponding to the matching proper time τ_m , and compare the result to a highly-accurate reference value computed using the mode-sum regularization method [33]. Similarly, in Fig. 4 we plot Φ_R as a function of the parameter ℓ_{cut} in the smoothing factor in the ℓ -sum (see Sec. II). Both figures show that the calculation of Φ_R via Eq. (29) is much better when replacing G_ℓ^{ret} by $G_\ell^{\text{ret}} - G_\ell^{\text{d}}$ than without the replacement. In fact, from Fig. 3 it is apparent that by using $G_\ell^{\text{ret}} - G_\ell^{\text{d}}$ we have entirely removed the need for matching to the power series approximation to $V(x, x')$.

V. DISCUSSION

In this paper we have presented a proposal for facilitating the calculation of the retarded Green function in Schwarzschild space-time. The proposal essentially consists of decomposing the Green function into multipolar ℓ -modes and significantly improving the convergence of the sum by subtracting the modes of the direct part in the

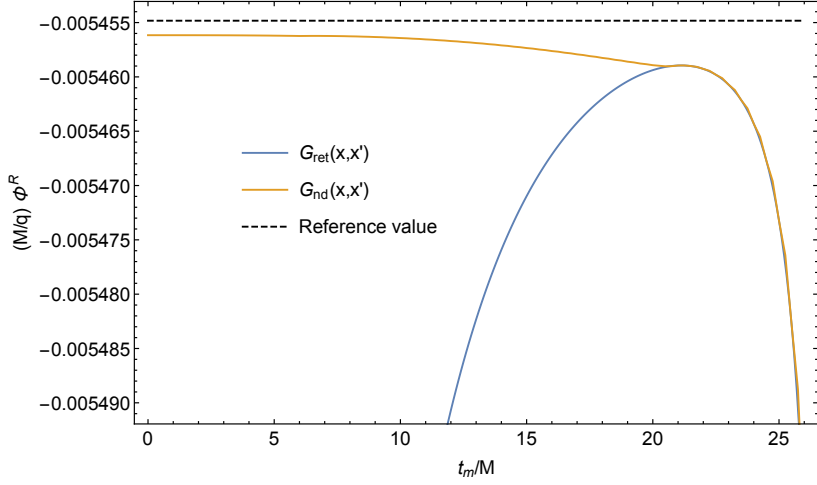


FIG. 3. Plot of the regularized self-field Φ_R [calculated via Eq. (29)] as a function of matching coordinate time t_m for a scalar charge on a circular geodesic at $r = 6M$. The solid blue line is obtained using Eq. (29) as it is (i.e., with G_ℓ^{ret} in the summand); the solid orange line is obtained using Eq. (29) with G_ℓ^{ret} replaced by $G_\ell^{\text{ret}} - G_\ell^{\text{d}}$ in the summand. In both cases the numerical integration was truncated at $t = 200M$, with the contribution for $t > 200M$ accounted for by a late-time approximation which assumes the branch-cut contribution to the GF dominates (see, e.g., [9, 10]). The dashed black line is a highly-accurate reference value computed using the mode-sum regularization method [33].

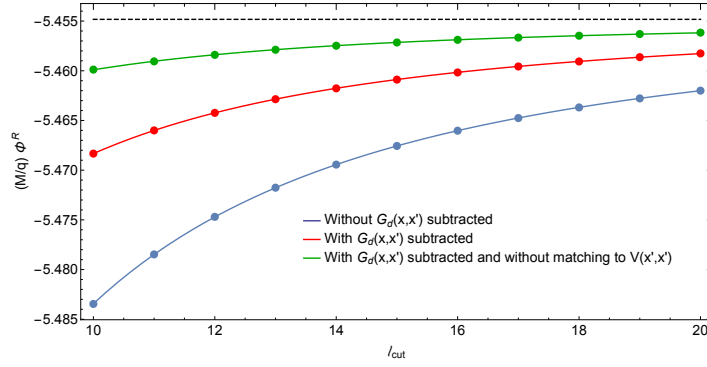


FIG. 4. The regularized self-field Φ_R for a scalar charge on a circular geodesic at $r = 6M$ as a function of the parameter ℓ_{cut} in the smoothing factor in the ℓ -sum (see Sec. II). Blue curve: Φ_R is calculated via Eq. (29) with $\tau_m = 18M$. Red curve: Φ_R is calculated via Eq. (29) with $\tau_m = 18M$ and with G_ℓ^{ret} replaced by $G_\ell^{\text{ret}} - G_\ell^{\text{d}}$. Green curve: Φ_R is calculated via Eq. (29) with $\tau_m = 0$ and with G_ℓ^{ret} replaced by $G_\ell^{\text{ret}} - G_\ell^{\text{d}}$.

Hadamard form. We have applied this method to the case of a scalar charge and its self-field. We next discuss various interesting extensions of this proposal and its applications.

First of all, we have applied this proposal to the calculation of the self-field, but the calculation could be extended to the calculation of the self-force. This requires calculating directly derivatives of the Green function, and so – from Eq. (20) – derivatives of the van Vleck determinant and the world function in the 2-D conformal spacetime \mathcal{M}_2 . A transport equation prescription for obtaining derivatives of both the world function and the van Vleck determinant are provided in [27].

Secondly, the proposal is readily generalizable from the zero-spin field considered here to higher-spin fields, such as the electromagnetic field or the linear gravitational field. These higher-spin fields in Schwarzschild space-time can be shown to satisfy a similar wave equation to the (scalar) Klein-Gordon equation, merely with a change in the potential (but not in the derivative terms). This implies that the retarded Green functions for these higher-spin wave equations also admit the Hadamard form Eq. (2), with just a change in the biscalar $V(x, x')$, but with the same world function σ and biscalar $U(x, x')$. It also implies that a conformal relationship similar to Eq. (7) between the Green functions in Schwarzschild and conformal Schwarzschild space-times is satisfied for these higher-spin fields. Therefore,

our proposed Eq. (22) also holds for these higher-spin cases, with the modes G_ℓ^{ret} and G_ℓ^{d} satisfying similar $(1+1)$ -D wave equations as in the scalar case, but with different potentials.

Finally, in this paper we have focused on dealing with the singularity which the Green function possesses at $\sigma = 0$, i.e., due to the “direct” null geodesic or at coincidence. However, as mentioned, the Green function diverges when the points are connected by *any* null geodesic, even if it is not the direct one. In [11], the full (i.e., including leading and subleading orders), global singularity structure of the Green function in Schwarzschild space-time was provided (the leading order had been previously provided in [34–37]). When multipole-decomposing the Green function, these non-direct singularities also arise as divergences in the multipolar ℓ -sum. Similarly to what we have done in Eq. (22) for the direct singularity, one could carry out ℓ -mode decompositions of the non-direct singularities and subtract those from the ℓ -modes of the full Green function. One should note, however, that the non-direct divergences alternate between Dirac- δ distributions (such as for the direct divergence) and principal value distributions. For obtaining the ℓ -modes, one would therefore have to perform angular integrals of the principal value distribution instead of the Dirac- δ distribution. It is expected that the resulting ℓ -sum would then converge everywhere, thus greatly facilitating further the calculation of the Green function. Regarding the subtracted non-direct divergences, one could include them separately by calculating them using, e.g., the expressions in [11]. Alternatively, if one is mainly interested in the calculation of the self-field/force, which involves worldline-integrals of the Green function, one could subtract only the part of the divergences which integrates to zero (i.e., with the coefficients of the diverging functions, such as the principal value, evaluated at the times of the divergences), instead of the full divergences (where the coefficients depend on time and so it would not integrate out to zero).

ACKNOWLEDGEMENTS

M. C. acknowledges partial financial support by CNPq (Brazil), process number 310200/2017-2. This work makes use of the Black Hole Perturbation Toolkit [38].

Appendix A: Series expansions of geometric quantities in \mathcal{M}_2

Equation (25) was obtained by substituting the expansion of the geometrical quantities $\epsilon\eta^2$ and $\Delta_{2d}^{1/2}$ through order $(\Delta x^a)^6$ into Eq. (20). For completeness we present these below; higher terms through $(\Delta x^a)^{20}$ are provided electronically as supplemental material to this paper.

$$\begin{aligned}
\epsilon\eta^2 = & -\frac{\Delta t^2(r-2M)}{r^3} + \frac{\Delta r^2}{r(r-2M)} + \frac{\Delta r\Delta t^2(r-3M)}{r^4} + \frac{\Delta r^3(r-M)}{r^2(r-2M)^2} - \frac{\Delta t^4(r-2M)(r-3M)^2}{12r^7} \\
& - \frac{\Delta r^2\Delta t^2(5r^2-28Mr+33M^2)}{6r^5(r-2M)} + \frac{\Delta r^4(11r^2-22Mr+15M^2)}{12r^3(r-2M)^3} + \frac{\Delta r\Delta t^4(2r^3-20Mr^2+63M^2r-63M^3)}{12r^8} \\
& + \frac{\Delta r^3\Delta t^2(4r^3-31Mr^2+67M^2r-45M^3)}{6r^6(r-2M)^2} - \frac{\Delta r^5(10r^3-30Mr^2+41M^2r-21M^3)}{12r^4(r-2M)^4} \\
& - \frac{\Delta t^6(r-3M)^2(r-2M)(4r^2-30Mr+45M^2)}{360r^{11}} - \frac{\Delta t^4\Delta r^2(78r^4-1072Mr^3+5087M^2r^2-10050M^3r+7065M^4)}{360r^9(r-2M)} \\
& - \frac{\Delta t^2\Delta r^4(64r^4-606Mr^3+1781M^2r^2-2160M^3r+945M^4)}{120r^7(r-2M)^3} \\
& + \frac{\Delta r^6(274r^4-1096Mr^3+2251M^2r^2-2310M^3r+945M^4)}{360r^5(r-2M)^5} + O((\Delta x^a)^7),
\end{aligned} \tag{A1}$$

$$\begin{aligned}
\Delta_{2d}^{1/2} = & 1 + \frac{\Delta t^2(21M^2 - 11Mr + r^2)}{6r^4} + \frac{\Delta r^2(15M^2 - 11Mr + r^2)}{6r^2(r - 2M)^2} - \frac{\Delta r \Delta t^2(4r^3 - 69Mr^2 + 290M^2r - 342M^3)}{24(r - 2M)r^5} \\
& + \frac{\Delta r^3(4r^3 - 69Mr^2 + 194M^2r - 162M^3)}{24r^3(r - 2M)^3} + \frac{\Delta t^4(r - 2M)(118r^3 - 2111Mr^2 + 9915M^2r - 13680M^3)}{2160r^8} \\
& + \frac{\Delta r^2 \Delta t^2(17r^4 - 368Mr^3 + 2246M^2r^2 - 5064M^3r + 3798M^4)}{108r^6(r - 2M)^2} \\
& + \frac{\Delta r^4(38r^4 - 897Mr^3 + 3887M^2r^2 - 6610M^3r + 3960M^4)}{240r^4(r - 2M)^4} \\
& - \frac{\Delta t^4 \Delta r(1016r^4 - 24575Mr^3 + 178346M^2r^2 - 500670M^3r + 477180M^4)}{8640r^9} \\
& + \frac{\Delta t^2 \Delta r^3(644r^5 - 16251Mr^4 + 125706M^2r^3 - 402955M^3r^2 + 571830M^4r - 298890M^5)}{4320r^7(r - 2M)^3} \\
& + \frac{\Delta r^5(432r^5 - 12973Mr^4 + 76588M^2r^3 - 198220M^3r^2 + 240300M^4r - 112140M^5)}{2880r^5(r - 2M)^5} \\
& + \frac{\Delta t^6}{1814400r^{12}}(29784r^6 - 873125Mr^5 + 9135623M^2r^4 - 46052780M^3r^3 \\
& \quad + 121262184M^4r^2 - 160751520M^5r + 84741660M^6) \\
& + \frac{\Delta t^4 \Delta r^2}{1814400r^{10}(r - 2M)^2}(304256r^6 - 9729943Mr^5 + 106098469M^2r^4 - 541361342M^3r^3 \\
& \quad + 1415223126M^4r^2 - 1839339360M^5r + 942984720M^6) \\
& + \frac{\Delta t^2 \Delta r^4}{1814400r^8(r - 2M)^4}(258392r^6 - 7409415Mr^5 + 68633901M^2r^4 - 281552428M^3r^3 \\
& \quad + 576945480M^4r^2 - 582918120M^5r + 232438140M^6) \\
& + \frac{\Delta r^6}{201600r^6(r - 2M)^6}(28752r^6 - 1049773Mr^5 + 7880183M^2r^4 - 27503250M^3r^3 \\
& \quad + 50452170M^4r^2 - 47416440M^5r + 18078120M^6) + O((\Delta x^a)^7). \tag{A2}
\end{aligned}$$

In order to obtain Eq. (25), we evaluated (A1) and (A2) for $\epsilon = -1$, $r = 6M$ and $\Delta r = 0$, inserted them in Eq. (20) and re-expanded for small Δt .

Appendix B: Bessel function expansion of G_ℓ^{ret}

At early times, it is useful to have an analytic approximation to G_ℓ^{ret} . This is easily obtained using a small modification of the method described in Ref. [32]. In particular, we start from the quantity $B(r, r')$ (which also depends on ω and ℓ defined in Eq. (2.13) of Ref. [32]). Starting from the expansion of $B(r, r')$ in powers of $r' - r$ and $\chi(r) \equiv [\omega^2 r^4 + r^2 f(r)(\ell + \frac{1}{2})^2]^{1/2}$ derived in that paper, we skip the sum over ℓ and proceed directly to the inverse Fourier transform. This amounts to computing integrals over frequency ω of the form

$$\int_0^\infty \chi^{-n-\frac{1}{2}} \cos(\omega \Delta t) d\omega = -\frac{(-1)^n \sqrt{\pi} (i \Delta t)^n}{r^{3n+2} f^{n/2} (2\ell + 1)^n \Gamma(n + \frac{1}{2})} I_n \left[\frac{\sqrt{f} (2\ell + 1)}{2r} i \Delta t \right] \tag{B1}$$

where n is a non-negative integer and $I_n(x)$ is the modified Bessel function of the first kind. The result is an expression for $B(r, r')$ (and thus G_ℓ^{ret}) as an infinite series of Bessel functions. Including a given number, n , of terms in the series yields a result which is accurate through $\mathcal{O}(\Delta t^{2n})$ (note, however, that it is better to keep the Bessel function form as that gives a more accurate result over a larger range of values for Δt). Explicitly, in the case $r = r'$ the first few

terms are

$$\begin{aligned}
G_\ell^{\text{ret}} = & \frac{1}{2}I_0 - \frac{i\Delta t I_1}{8(2\ell+1)r^2}\sqrt{f}(r-8M) + \frac{\Delta t^2 I_2}{192(2\ell+1)^2r^5}\left[32(30\ell^2+30\ell-79)M^2r - 2(320\ell^2+320\ell-219)Mr^2 \right. \\
& + 3(32\ell^2+32\ell-1)r^3 + 3456M^3\left] - \frac{i\Delta t^3 I_3}{3840\sqrt{f}(2\ell+1)^3r^8}\left[11520(54\ell^2+54\ell-281)M^4r + 160(72\ell^4+144\ell^3 \right. \\
& - 5044\ell^2-5116\ell+10191)M^3r^2 - 4(3360\ell^4+6720\ell^3-91280\ell^2-94640\ell+86013)M^2r^3 + 4(1280\ell^4 \\
& + 2560\ell^3-16464\ell^2-17744\ell+6275)Mr^4 - 5(128\ell^4+256\ell^3-736\ell^2-864\ell+1)r^5 + 2304000M^5\left] + \dots, \tag{B2}
\end{aligned}$$

where the argument of all the Bessel functions is the same as that of I_n in Eq. (B1). In this work, we make use of an expansion through $n = 20$; the higher terms are provided electronically as supplemental material to this paper. In order to obtain Eq. (24), we evaluated (B2) for $r = 6M$ and expanded for small Δt .

-
- [1] E. Poisson, A. Pound, and I. Vega, Living Rev. Rel. **14**, 7 (2011), 1102.0529.
 - [2] B. Wardell and A. Gopakumar, Fund. Theor. Phys. **179**, 487 (2015), 1501.07322.
 - [3] R. H. Jonsson, E. Martín-Martínez, and A. Kempf, Physical review letters **114**, 110505 (2015).
 - [4] A. Blasco, L. J. Garay, M. Martín-Benito, and E. Martín-Martínez, Physical review letters **114**, 141103 (2015).
 - [5] P. R. Garabedian, *Partial Differential Equations* (Chelsea Pub Co, New York, 1998), ISBN 9780821813775.
 - [6] M. Ikawa, *Hyperbolic partial differential equations and wave phenomena. Iwanami series in modern mathematics. Translations of mathematical monographs* (American Mathematical Soc., Providence, 2000), ISBN 9780821810217.
 - [7] J. Hadamard, *Lectures on Cauchy's Problem in Linear Partial Differential Equations* (Dover Publications, 1923), ISBN 978-0486495491.
 - [8] F. G. Friedlander, *The Wave Equation on a Curved Space-time* (Cambridge University Press, Cambridge, 1975), ISBN 978-0521205672.
 - [9] M. Casals, S. Dolan, A. C. Ottewill, and B. Wardell, Phys. Rev. D **88**, 044022 (2013).
 - [10] B. Wardell, C. R. Galley, A. Zenginoğlu, M. Casals, S. R. Dolan, and A. C. Ottewill, Phys. Rev. D **89**, 084021 (2014).
 - [11] M. Casals and B. Nolan, arXiv preprint arXiv:1606.03075 (2016).
 - [12] J. L. Synge, *Relativity: The General Theory* (North-Holland, Amsterdam, 1960), ISBN 978-0720400663.
 - [13] J. H. Van Vleck, Proc. Nat. Acad. Sci. **14**, 178 (1928).
 - [14] C. Morette, Phys. Rev. **81**, 848 (1951).
 - [15] M. Visser, Phys. Rev. D **47**, 2395 (1993).
 - [16] M. Casals, C. Kavanagh, A. C. Ottewill, and B. Wardell, in preparation.
 - [17] E. W. Leaver, Phys. Rev. D **34**, 384 (1986).
 - [18] Z. Mark, A. Zimmerman, S. M. Du, and Y. Chen, Phys. Rev. **D96**, 084002 (2017), 1706.06155.
 - [19] G. Hardy, *Divergent Series* (Oxford Clarendon Press, 1949), ISBN 978-0-8218-2649-2.
 - [20] E. Poisson and A. G. Wiseman, *Suggestion at the 1st Capra ranch meeting on radiation reaction* (1998).
 - [21] W. G. Anderson and A. G. Wiseman, Class. Quantum Grav. **22**, S783 (2005), gr-qc/0506136.
 - [22] M. Casals, S. Dolan, A. C. Ottewill, and B. Wardell, Phys. Rev. **D79**, 124043 (2009), 0903.0395.
 - [23] A. C. Ottewill and B. Wardell, Phys. Rev. **D77**, 104002 (2008), 0711.2469.
 - [24] M. Casals and B. C. Nolan, Phys. Rev. D **92**, 104030 (2015).
 - [25] N. Birrell and P. Davies, *Quantum Fields in Curved Space* (Cambridge University Press, Cambridge, 1984).
 - [26] M. Casals and B. C. Nolan, Phys.Rev. **D86**, 024038 (2012), 1204.0407.
 - [27] A. C. Ottewill and B. Wardell, Phys.Rev. **D84**, 104039 (2011), 0906.0005.
 - [28] C. R. Galley and B. Wardell, in preparation.
 - [29] *GreenFunctionSurrogate Mathematica package*, (bhptoolkit.org/GreenFunctionSurrogate).
 - [30] D. Q. Aruquipa and M. Casals, in preparation.
 - [31] C. O'Toole, A. C. Ottewill, and B. Wardell, in preparation.
 - [32] M. Casals, S. Dolan, A. C. Ottewill, and B. Wardell, Phys. Rev. **D79**, 124044 (2009), 0903.5319.
 - [33] A. Heffernan, A. Ottewill, and B. Wardell, Phys. Rev. **D86**, 104023 (2012), 1204.0794.
 - [34] A. Ori, private communication (2008) and report (2009) available at <http://physics.technion.ac.il/~amos/acoustic.pdf>.
 - [35] S. R. Dolan and A. C. Ottewill, Phys. Rev. **D84**, 104002 (2011), 1106.4318.
 - [36] A. I. Harte and T. D. Drivas, Physical Review D **85**, 124039 (2012).
 - [37] A. Zenginoğlu and C. R. Galley, Phys. Rev. D **86**, 064030 (2012), 1206.1109.
 - [38] *Black Hole Perturbation Toolkit*, bhptoolkit.org.